




# Microstructure and mechanical properties of TC4 joints brazed with Ti–Zr–Cu–Sn amorphous filler alloy

Hui-Hui Zhang, Zhen-Duo Cui, Sheng-Li Zhu\* , Shi-Wei Guo, Xian-Jin Yang, Akihisa Inoue

Received: 17 September 2018/Revised: 22 October 2018/Accepted: 16 April 2020/Published online: 30 May 2020  
© The Nonferrous Metals Society of China and Springer-Verlag GmbH Germany, part of Springer Nature 2020

**Abstract** The  $\text{Ti}_{51.44}\text{Zr}_{16.26}\text{Cu}_{30}\text{Sn}_{2.3}$  (at%) amorphous filler alloy in a ribbon form was prepared by melt spinning. The Ti–6Al–4V alloy was brazed in vacuum furnace by using the  $\text{Ti}_{51.44}\text{Zr}_{16.26}\text{Cu}_{30}\text{Sn}_{2.3}$  amorphous filler alloy. The effects of brazing temperature and holding time on the interfacial microstructure and mechanical properties of the Ti–6Al–4V brazed joints were investigated. The brazed joints are composed of  $\alpha$ -Ti,  $\beta$ -Ti, and (Ti, Zr)<sub>2</sub>Cu phases. The shear strength of the joints increases with brazing temperature increasing from 1153 to 1193 K and holding time from 10 to 15 min, while decreases with brazing temperature and time further increasing. Low temperature brazing results in the formation of microcracks and voids in the seams, which are harmful for the shear strength of the joints. In the joint brazed at 1193 K for 15 min, a fine  $\alpha + \beta$  Widmanstätten structure beneficial to the mechanical property is formed, and the joint exhibits relatively high joint strength of 180 MPa.

**Keywords** Amorphous alloy; Brazing; Titanium alloy; Microstructure; Mechanical property

## 1 Introduction

Titanium (Ti) alloys are the most promising structural materials with the purpose of weight reduction and corrosion control [1, 2]. Among them, Ti–6Al–4V (TC4) is considered as the most important Ti alloy in many fields, such as biomaterials, and aerospace and aviation materials. It was reported that TC4 alloy had captured about 60% of the titanium alloys market during the approximately past 60 years [2, 3]. TC4 alloy consists of  $\alpha$  and  $\beta$  allotropic phases. The  $\beta$ -transus temperature ( $T_{\beta}$ , transformation from  $\alpha$  to  $\beta$ ) of TC4 is known as 1268 K [2–7]. Therefore, for joining TC4 alloy, reasonable joining technologies with a joining temperature lower than the  $\beta$ -transus temperature are required in order to avoid the phase transformation and mechanical property impairment of the base materials [8]. Compared with welding, brazing has many advantages including little influence on the base materials, residual stress reduction, and control of brittle phases [1, 4, 5, 9]. Ag-based, Al-based and Ti-based filler metals have been reported for joining Ti alloys [5, 10]. The relatively lower mechanical stability and bonding strength of the Ti alloy joints brazed with Ag-based and Al-based filler metals limit their applications [10–12]. The joints brazed with Ti-based filler metals commonly show high bonding strength due to the good chemical compatibility between the fillers and the Ti alloy substrates [2, 10, 13, 14]. However, high melting temperature of filler metals would result in high cost in the brazing process. Amorphous alloys, as a kind of metastable materials, are promising brazing materials due to low melting temperatures and good viscous

---

H.-H. Zhang, Z.-D. Cui, S.-L. Zhu\*, S.-W. Guo, X.-J. Yang, A. Inoue  
School of Materials Science and Engineering, Tianjin University, Tianjin 30007, China  
e-mail: slzhu@tju.edu.cn

Z.-D. Cui, S.-L. Zhu  
Key Laboratory of Advanced Ceramics and Machining Technology, Ministry of Education, Tianjin 300072, China

S.-L. Zhu, X.-J. Yang  
Tianjin Key Laboratory of Composite and Functional Materials, Tianjin 300072, China

A. Inoue  
Department of Physics, King Abdulaziz University, Jeddah 22254, Saudi Arabia

flow ability during brazing process [13, 15, 16]. Compared with crystalline brazing filler metals commonly in wire, strip, powder and paste forms, amorphous brazing filler metals in a ribbon form prepared by melt spinning show some significant advantages. Amorphous brazing filler metals can be easily fabricated into continuous ribbons so that they can be used in a preplaced preform with a minimal and accurate amount in the joint clearances. They also exhibit high homogeneity in structure and composition and high purity, which are favorable for high mechanical properties of the joints [4]. In addition, it has been reported that amorphous alloys improve metal atomic diffusion and interfacial reaction due to their metastable state [17, 18]. Hence, Ti-based amorphous alloys are considered as a good substitute for the traditional filler metals for Ti alloys [15, 18, 19].

In the present study, we prepared  $\text{Ti}_{51.44}\text{Zr}_{16.26}\text{Cu}_{30}\text{Sn}_{2.3}$  (at%) amorphous alloy ribbon by using a melt-spinning method. High-vacuum brazing was applied to join Ti-6Al-4V alloy using the as-prepared  $\text{Ti}_{51.44}\text{Zr}_{16.26}\text{Cu}_{30}\text{Sn}_{2.3}$  amorphous alloy ribbon. Microstructure and mechanical properties of the joints were investigated systematically.

## 2 Experimental

The TC4 alloy was cut to the samples with a dimension of  $10\text{ mm} \times 10\text{ mm} \times 3\text{ mm}$ . The microstructure of the original TC4 alloy is shown in Fig. 1. The original TC4 is composed of two phases, hcp  $\alpha$  phase (gray) and bcc  $\beta$  phase (black) [20, 21]. Before brazing, the TC4 samples were polished with waterproofed sandpaper following ultrasonic cleaning in acetone. The  $\text{Ti}_{51.44}\text{Zr}_{16.26}\text{Cu}_{30}\text{Sn}_{2.3}$  (at%) amorphous alloy ribbon with a thickness of  $50\ \mu\text{m}$  and a width of  $10\text{ mm}$  was prepared by melt-spinning method. The amorphous nature of the ribbon was determined by an X-ray diffractometer (XRD, Bruker D8) with

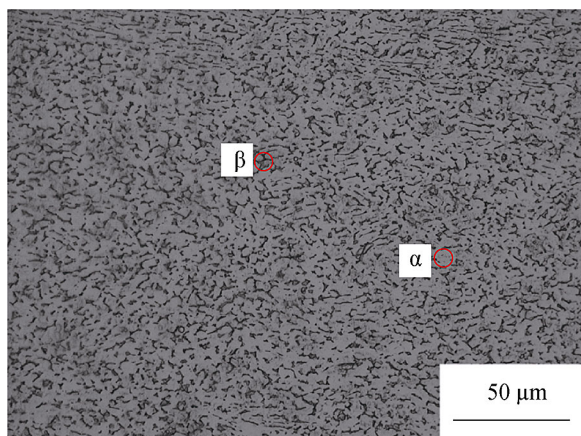


**Fig. 1** OM image of TC4 base metal

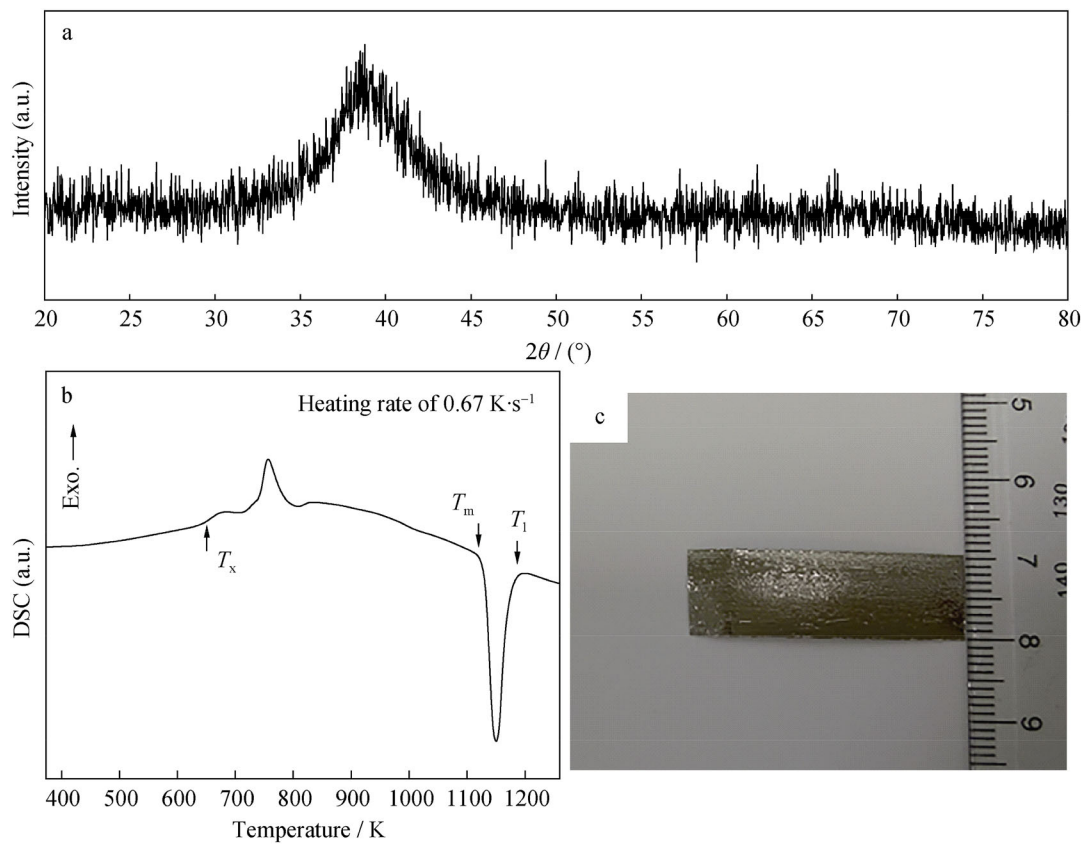
Cu  $K\alpha$  radiation. The thermal behavior of the ribbon was measured by differential scanning calorimetry (DSC, Mettler-Toledo STD1600) at a heating rate of  $0.67\ \text{K}\cdot\text{s}^{-1}$ .

The amorphous ribbon was cleaned using acetone before assembling and then sandwiched between the overlapped area ( $10\text{ mm} \times 10\text{ mm}$ ) of the TC4 base metals. The braze process was carried out under high-vacuum atmosphere. The brazing temperatures were in the range of  $1153\text{--}1213\text{ K}$ , which were lower than the  $\alpha$ - $\beta$  transformation temperature ( $1268\text{ K}$ ) of TC4 alloy [22, 23]. Samples of brazed joints were longitudinally cut and prepared by standard grinding and polishing procedure. For microscopic analyses of the brazed joints, the brazed samples were etched in a mixed solution of  $2\text{ ml}$  HF solution ( $50\text{ wt.}\%$ ),  $4\text{ ml}$   $\text{HNO}_3$  solution ( $67\text{ wt.}\%$ ) and  $100\text{ ml}$  deionized  $\text{H}_2\text{O}$ . The microstructure, compositions and phases were characterized by optical microscope (OM, Leica DM 2700 M), scanning electron microscopy (SEM, Hitachi S4800) coupled with an energy-dispersive X-ray spectrometer (EDS, JSM 7800F), and XRD. The hardness was tested by a Vickers microhardness tester (Wilson, Tukon<sup>tm</sup> 1202) with a load of  $0.49\text{ N}$ . The compressive shear tests of the brazed joints were performed using a mechanical testing machine at a compression speed of  $1\text{ mm}\cdot\text{s}^{-1}$ .

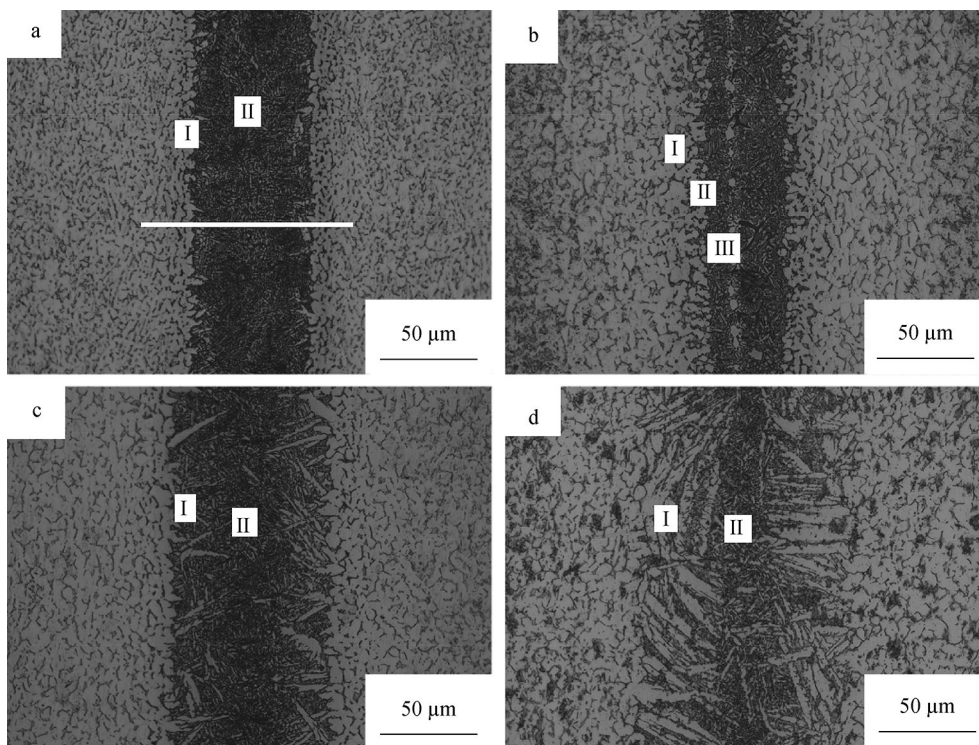
## 3 Results and discussion

Figure 2a shows XRD pattern of  $\text{Ti}_{51.44}\text{Zr}_{16.26}\text{Cu}_{30}\text{Sn}_{2.3}$  ribbon. There is only a broad halo without any sharp peaks corresponding to crystalline phases, indicating amorphous nature of the ribbon. Figure 2b shows DSC curve of the  $\text{Ti}_{51.44}\text{Zr}_{16.26}\text{Cu}_{30}\text{Sn}_{2.3}$  ribbon, which exhibits two characteristic exothermic peaks corresponding to successive multi-stage crystallization events [24]. The melting temperature ( $T_m$ ), liquidus temperature ( $T_l$ ) and crystallization temperature ( $T_x$ ) of the  $\text{Ti}_{51.44}\text{Zr}_{16.26}\text{Cu}_{30}\text{Sn}_{2.3}$  ribbon are determined as  $1129$ ,  $1173$  and  $651\text{ K}$ , respectively. DSC curve in Fig. 2b exhibits almost single endothermic peak, which implies that the  $\text{Ti}_{51.44}\text{Zr}_{16.26}\text{Cu}_{30}\text{Sn}_{2.3}$  should be of eutectic or near-eutectic composition. The macroscopic view of  $\text{Ti}_{51.44}\text{Zr}_{16.26}\text{Cu}_{30}\text{Sn}_{2.3}$  amorphous filler metals is shown in Fig. 2c.

Figure 3 shows OM images of cross sections of the samples brazed at different temperatures in the range of  $1153\text{--}1213\text{ K}$  for  $15\text{ min}$ , showing that the TC4 alloy and the filler metal are tightly bonded together. The thickness of the brazed seams is about  $110$ ,  $125$ ,  $130$  and  $150\ \mu\text{m}$  for the brazing temperatures of  $1153$ ,  $1173$ ,  $1193$  and  $1223\text{ K}$ , respectively. With brazing temperature increasing, the elemental diffusion and interfacial reaction should become more active, resulting in wider brazing seams. There are



**Fig. 2** a XRD pattern, b DSC curve and c macroscopic view of  $Ti_{51.44}Zr_{16.26}Cu_{30}Sn_{2.3}$  (at%) amorphous filler metal



**Fig. 3** OM images of TC4 joints brazed for 15 min at a 1153 K, b 1173 K, c 1193 K and d 1213 K



three typical areas in each seam: diffusion Layer I that is adjacent to the TC4 substrate, discontinuous reaction Layer II and the central Layer III. At 1153 K, the TC4 substrate keeps original fine structure and Layer I is very thin, indicating that elemental diffusion and interfacial reaction are insufficient. At 1173 K, the microstructure of Layer I is similar to that of the TC4 substrate, Layer II consists of more equiaxed  $\alpha$  phase, and Layer III is separate phase. At the temperatures of 1193 and 1213 K,  $\alpha$  phase in the joints exhibits acicular morphology, and Layer I consists of acicular  $\alpha$  phase and intergranular  $\beta$  phase [3, 10].

Because the brazing temperature is higher than the melting point of the filler alloy, the filler alloy would be molten during the brazing process. At the early stage of brazing, the TC4 alloy would partially dissolve into the molten filler alloy. Obviously, the TC4 alloy contains more Ti than the filler alloy. In the seam, the area near the TC4 should become richer in Ti. Because the brazing temperature is lower than the  $\alpha$ - $\beta$  transformation temperature,  $\alpha$ -Ti should preferentially nucleate and grow out of the  $\beta$  phase at the TC4 substrate toward the center of the brazed seam. The morphology of  $\alpha$ -Ti in the seam changes from equiaxed to acicular, as shown in Layer I. Cu and Zr atoms

would be expelled from the growing  $\alpha$ -Ti phase and dispersed  $(\text{Ti, Zr})_2\text{Cu}$  phases ( $\gamma$ ) would be formed, Sn exists as  $\alpha$  reinforced phase [13]. In addition, because the solubility of Cu in  $\beta$ -Ti is higher than that in  $\alpha$ -Ti [25–27], Cu would partially enter the  $\beta$ -Ti phase during the subsequent growth of  $\alpha$ -Ti. The  $\beta$ -Ti phase would segregate and grow along  $\alpha$ -Ti phase by eutectoid transformations. Finally, there is the lamellar  $\beta$ -Ti between the two acicular  $\alpha$ -Ti phases. This structure is called “ $\alpha + \beta$  Widmanstätten structure”, which is formed in the late stage of brazing process, as shown in Fig. 3d. It is seen that the thickness of the Widmanstätten structure increases with the brazing temperature and time increasing. With temperature increasing, the grain size of TC4 matrix becomes larger, Layer I becomes thicker, and Layer II shrinks until nearly disappears. For the joint brazed at 1213 K,  $\alpha + \beta$  Widmanstätten structure distributes in the whole braze cross-section, as shown in Fig. 3d.

Figure 4 shows elemental distribution perpendicular to the seam (e.g., along the white line in Fig. 3a). For the joint brazed at 1153 K, there is a sharp change in Ti content between the substrate and joint. With the brazing temperature increasing, the changes in elemental contents tend to

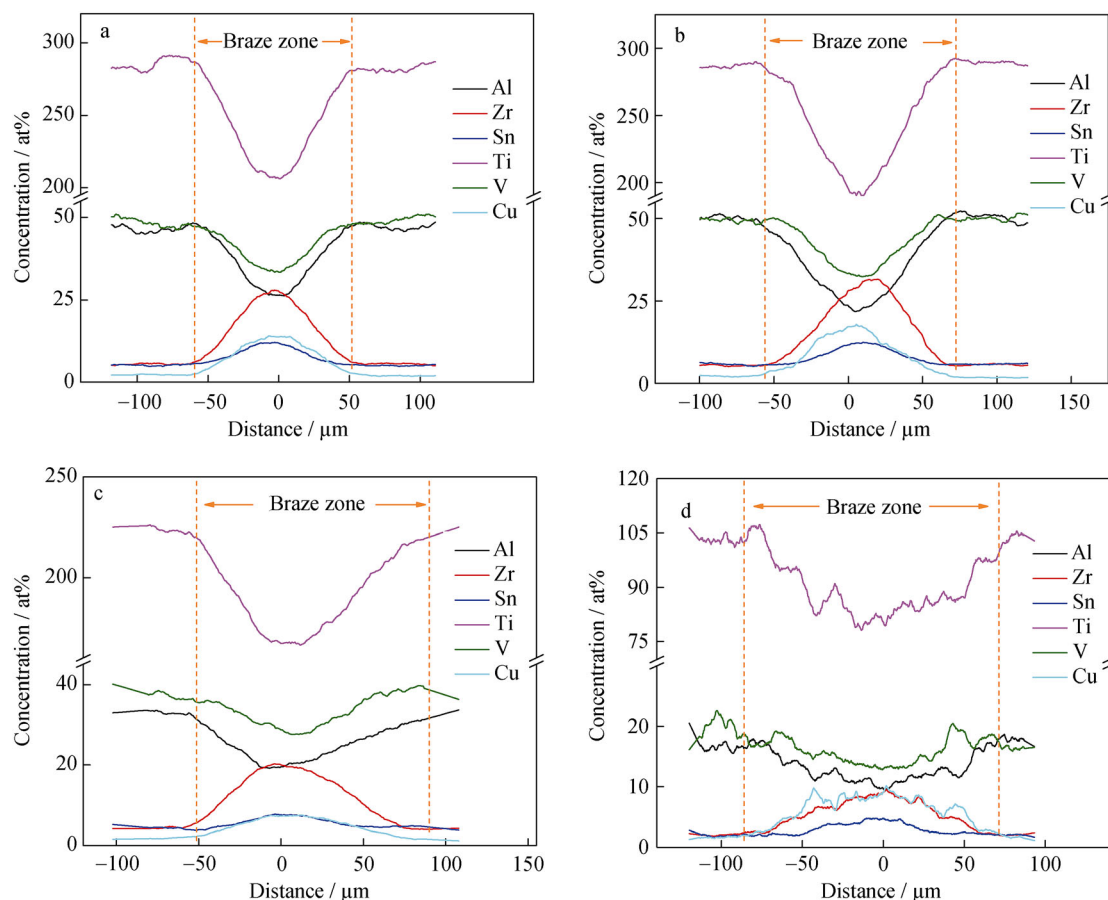


**Fig. 4** Elemental distribution along direction perpendicular to seam of joints brazed at **a** 1153 K, **b** 1173 K, **c** 1193 K and **d** 1213 K for 15 min

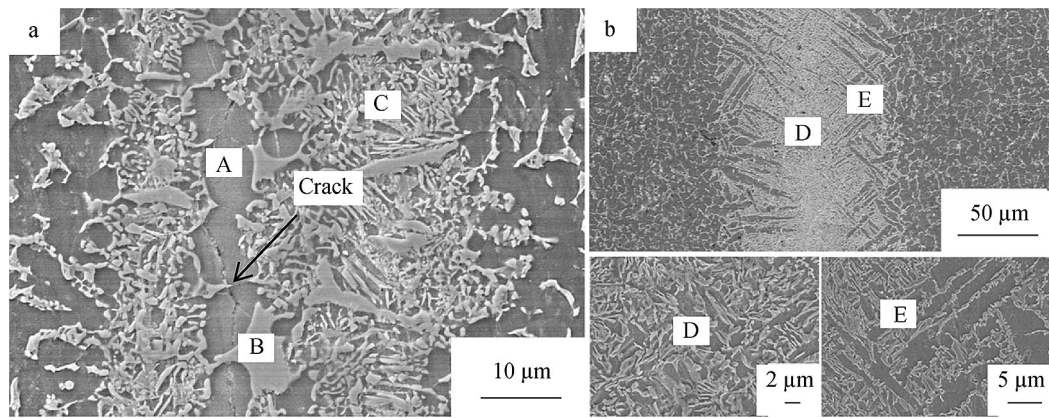


**Fig. 5** SEM images of joint interfaces brazed at **a** 1173 K and **b** 1213 K for 15 min

**Table 1** EDS analysis results in Regions A-E in Fig. 5

Temperature/K	Regions	Content/at%					Potential phase/s	
		Ti	Al	V	Zr	Cu		Sn
1173	A	87.3	5.6	0	3.4	2.2	1.5	$\alpha$ -Ti, (Ti, Zr) <sub>2</sub> Cu
	B	47.2	8.2	2.1	11.6	29.5	0.9	(Ti, Zr) <sub>2</sub> Cu
	C	66.5	7.9	1.9	6.1	16.5	1.1	$\alpha$ -Ti, (Ti, Zr) <sub>2</sub> Cu
1213	D	72.5	8.6	1.8	4.8	10.9	1.4	$\alpha$ -Ti, (Ti, Zr) <sub>2</sub> Cu
	E	78.4	11.2	1.9	1.6	6.4	0.5	$\alpha$ + $\beta$ Ti

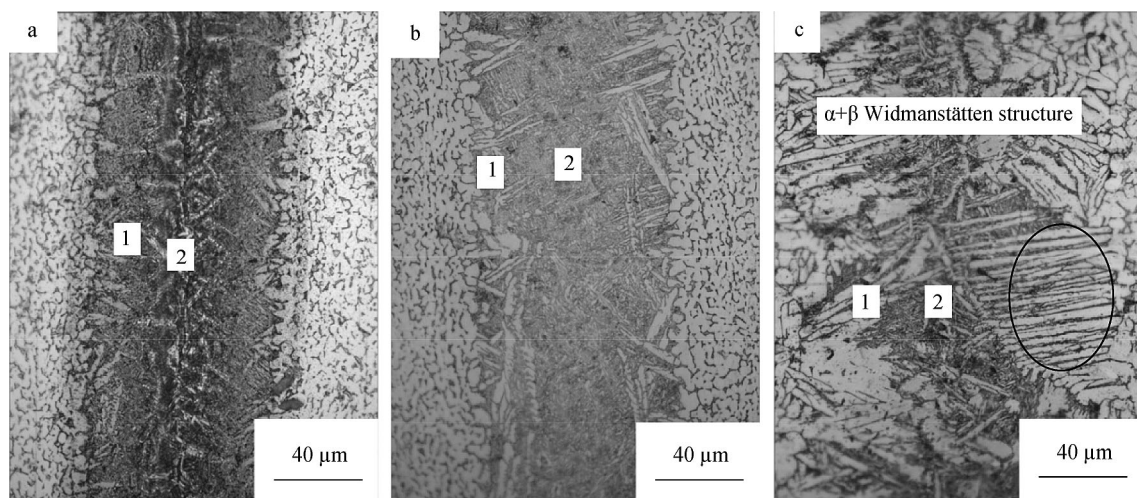


**Fig. 6** OM images of samples brazed at 1193 K for **a** 10 min, **b** 15 min and **c** 20 min

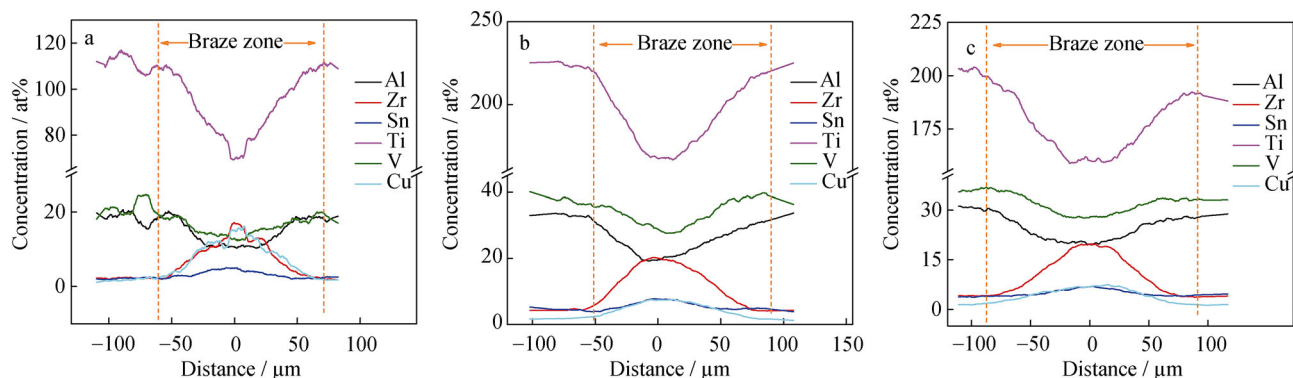
be gentle and the diffusion layer becomes thicker. In addition, cracks and separate phases are found in the samples brazed at relative lower temperatures, as shown in Fig. 3a, b. When the temperature rises to 1213 K (Fig. 4d), the brazing seam becomes inerratic and wider correspondingly, and only slight composition change is observed.

Figure 5a, b shows the enlarged images of Fig. 3b, d, respectively. The compositions of the regions with different morphologies marked as A, B, C, D, and E were examined by EDS. Combining elemental contents, Ti(Zr)-Al-Cu ternary alloy diagram and previous researches [13, 28, 29], and EDS results, the compositions and suggested phases of the regions are listed in Table 1. The TC4

substrate is primarily composed of  $\alpha$ -Ti and  $\beta$ -Ti phases. Layer I adjacent to TC4 substrate consists of high contents of Ti and Al, and low contents of Cu and Zr. For the sample subjected to the brazing at 1173 K for 15 min, three types of microstructure (marked as A, B and C) could be observed in the joint. The element pairs of Ti and Zr is not only chemically compatible, but also completely soluble to each other. Hence, both  $Zr_2Cu$  and  $Ti_2Cu$  can be collectively referred to as  $(Ti, Zr)_2Cu$  ( $\gamma$  phases) [4, 13]. Region A in Fig. 5a contains the highest content of Ti and very few Cu, which should be  $\alpha$ -Ti phase because of the lower solubility of Cu in  $\alpha$ -Ti than that in  $\beta$ -Ti. Region B in Fig. 5a contains higher contents of Cu and Zr, which should be brittle intermetallic compounds  $(Ti, Zr)_2Cu$ . In the brazing process, different phases have different linear shrinkage, which leads to residual thermal stress. Moreover, the residual thermal stress and the presence of brittle intermetallic compound  $(Ti, Zr)_2Cu$  in Region A would result in microcracks (Fig. 5a). Region C in Fig. 5a exhibits eutectoid microstructure, which should be composed of  $\alpha$ -Ti and  $(Ti, Zr)_2Cu$  phases [5]. In the sample subjected to brazing at 1213 K for 15 min, Region D is also eutectoid microstructure consisting of  $\alpha$ -Ti and  $(Ti, Zr)_2Cu$  phases,

and Region E presents the lamellar  $\alpha + \beta$  Widmanstätten structure (Fig. 5b).

Figure 6 shows cross-sectional images of the joints brazed at 1193 K for various time. Figure 7 shows relative elemental distribution perpendicular to the seam. There are two layers (marked with 1 and 2 in Fig. 6a) in the seam of the sample brazed for 10 min. The border of the seam is mainly composed of the original  $\beta$ -Ti in the substrate, in which some  $\alpha$ -Ti nucleates from the TC4 substrate. Figure 7a shows a sharp composition change in the center of the seam, and the composition of Layer 2 in Fig. 6a is close to the original composition of the filler alloy. Layer 2 is the residual filler alloy which locates in the center of joints. With the brazing time increasing, the degree of elemental dissolution, diffusion and interfacial reaction increases between TC4 substrate and the filler alloy, leading to the decrease in Zr, Cu and Sn contents and the increase in Ti, Al and V contents in the central region of the brazing joints. In addition, with brazing time increasing, the composition change along the direction perpendicular to the seam becomes gentle, as shown in Fig. 7b, c. This would result in more lamellar  $\alpha + \beta$  Widmanstätten structure due to sufficient eutectoid reaction at the brazing seam. The



**Fig. 7** Elemental distribution perpendicular to seam at 1193 K for **a** 10 min, **b** 15 min, and **c** 20 min

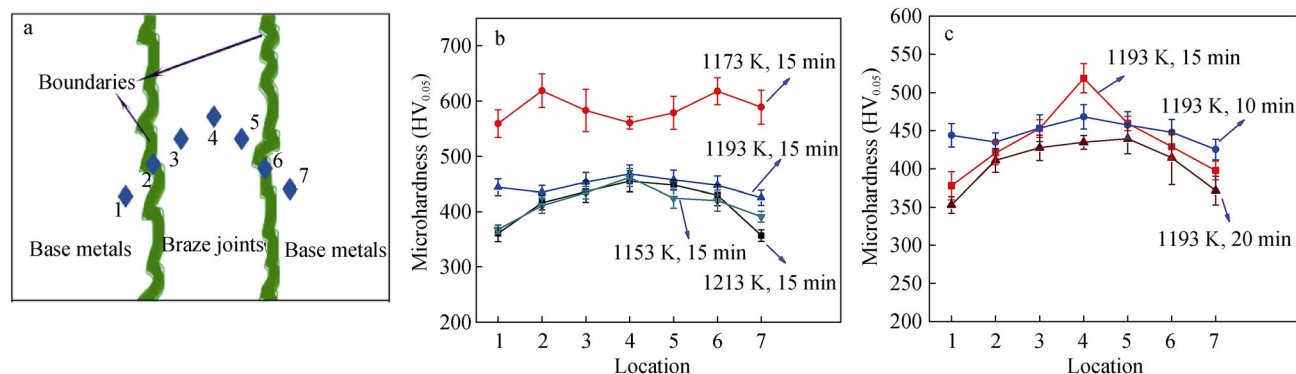


**Fig. 8** Vickers hardness test results: **a** test location diagram, **b** brazed at various temperature for 15 min and **c** brazed at 1193 K for various time



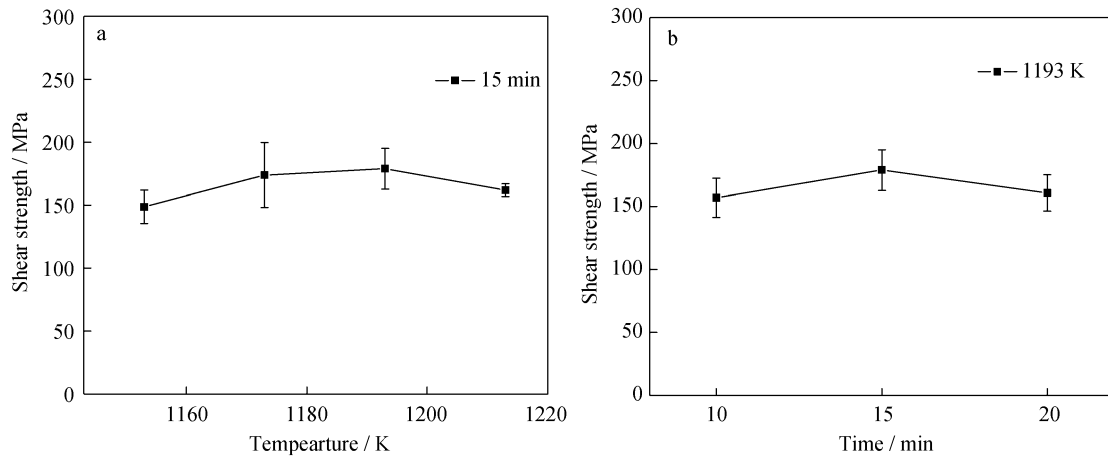


Fig. 9 Effect of a brazing temperature and b holding time on shear strength of brazed samples

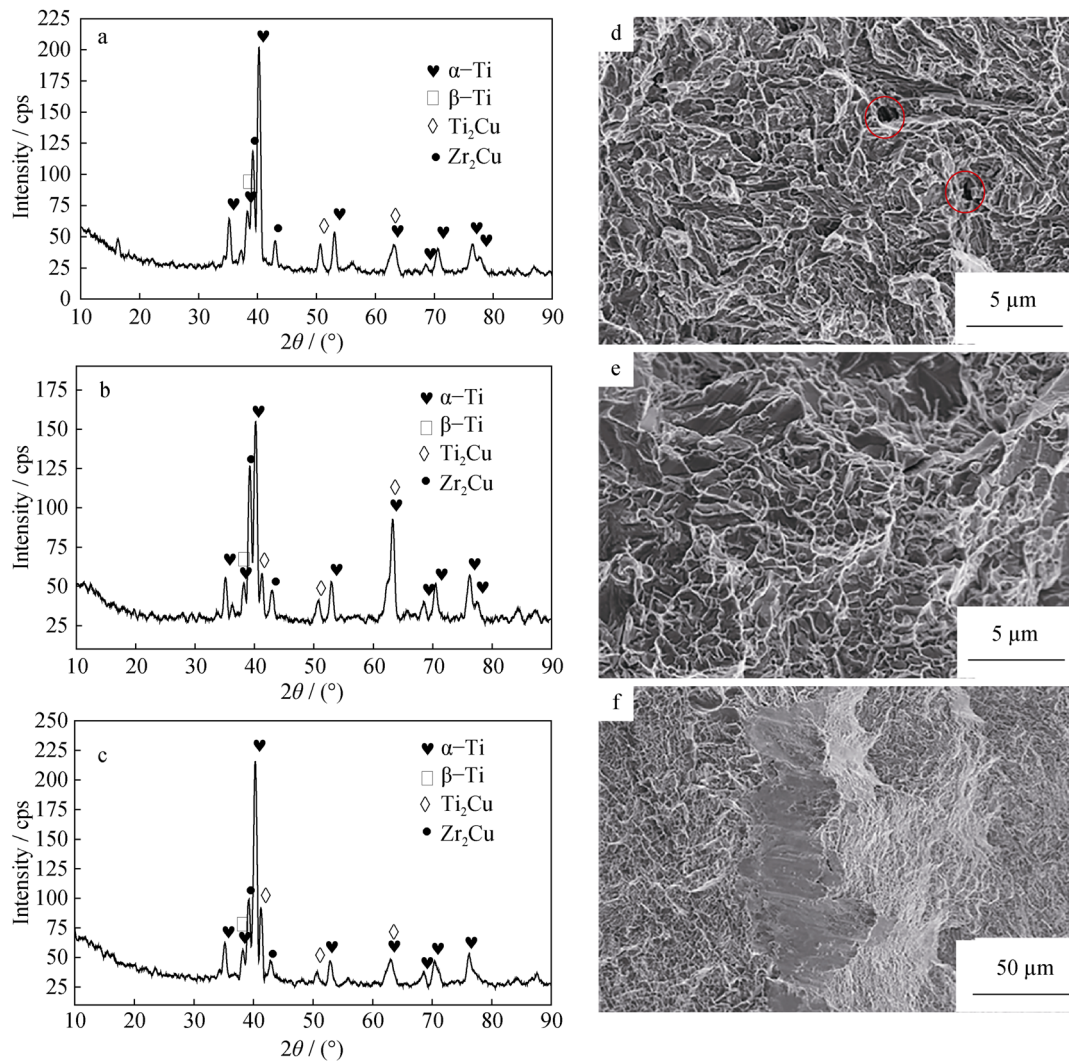


Fig. 10 XRD patterns and SEM images of fracture surface of samples brazed at a, d 1173 K for 15 min, b, e 1193 K for 15 min and c, f 1193 K for 10 min

black circle in Fig. 7c shows the obvious Widmanstätten structure.

Figure 8 shows the hardness test region diagram and the curves of Vickers hardness versus brazing temperature or brazing time. As shown in Fig. 8a, except the sample brazed at 1173 K, the highest hardness values locate in the center regions (Location 4). According to Fig. 4a and Table 1, for the sample brazed at 1173 K, Regions B and C contain a number of brittle intermetallic compounds (Ti, Zr)<sub>2</sub>Cu with very high hardness. It was reported that the existence of brittle intermetallic compounds would be inevitable [4]. Figure 8c shows Vickers hardness results of the samples brazed for various time at 1193 K. For the 10-min sample, the hardness exhibits larger change as a result of the insufficient element diffusion and interfacial reaction. With time increasing, the hardness changes gently. Further increase of brazing time would result in the grain growth, hence the hardness decreases.

Figure 9 shows shear strength of the brazed joints at room temperature. With the increase in both brazing temperature and time, the average shear strength increases firstly and then decreases. The increase in shear strength at first stage is due to the more sufficient atom diffusion and the formation of more lamellar  $\alpha + \beta$  Widmanstätten structure by the eutectoid reaction. It was reported that the braze joints consisting of only fine eutectoidal and Widmanstätten + eutectoidal microstructures would have outstanding mechanical properties [9]. The maximum shear strength of 180 MPa is obtained for the braze joints brazed at 1193 K for 15 min. The decrease in shear strength for the samples brazed at higher temperature with longer holding time should be caused by the formation of more brittle intermetallic compounds (Ti, Zr)<sub>2</sub>Cu [2, 4, 13].

Fractographic analysis is a useful and efficiency method for exploring crack nucleation and propagation [4]. The morphologies and XRD patterns of the fracture surface for the samples brazed at 1173 and 1193 K for 15 min, and at 1193 K for 10 min are shown in Fig. 10. XRD patterns confirm the existence of  $\alpha$ -Ti,  $\beta$ -Ti and (Ti, Zr)<sub>2</sub>Cu in the brazed joint, which is consistent with the microstructure analysis given above. Few Ti<sub>3</sub>Al distributes in the fracture surface of the joint brazed, which is common phase in the TiAl alloy without influence upon the properties of TC4 joints nearly. Some voids (marked with red circles) could be observed in the fracture surface of the joint brazed at 1173 K (Fig. 10a, d). In addition, for the sample brazed at 1173 K for 15 min, microcracks can be observed in Region A in Fig. 5a. These voids and microcracks would be the sources of cracks, and would result in the poor shear strength. According to EDS results shown in Table 1, the fracture should occur in Region A marked in Fig. 5a primarily. High brazing temperature and long brazing time would promote atom diffusion and interface reaction and

furthermore depress the formation of the defects, such as micro-gap and pore. Hence, the shear strength was improved by increasing brazing temperature and time. The fracture surface of the sample brazed at 1193 K for 10 min exhibits finer crystalline grain and obvious residual filler alloy in the center of the seam due to the insufficient diffusion and growth of  $\alpha$ -Ti, as shown in Fig. 10c, f. For all the samples, XRD patterns indicate that  $\alpha$ -Ti phase would dominate fractured surfaces.

## 4 Conclusion

In this paper, the Ti<sub>51.44</sub>Zr<sub>16.26</sub>Cu<sub>30</sub>Sn<sub>2.3</sub> (at%) amorphous filler alloy in a ribbon form was prepared by melt spinning. The TC4 alloy can be metallurgically bonded by using the Ti<sub>51.44</sub>Zr<sub>16.26</sub>Cu<sub>30</sub>Sn<sub>2.3</sub> amorphous filler alloy. Under appropriate conditions, lamellar  $\alpha + \beta$  Widmanstätten structure layer is formed at the brazed joints, which would favor the improvement of bonding strength. At relatively lower temperatures, such as 1153 and 1173 K, residual stress closed to the brittle intermetallic compound results in the formation of microcracks. The shear strength of the joints increases with brazing temperature increasing from 1153 to 1193 K and holding time from 10 to 15 min, while decreases with brazing temperature and time further increasing. The maximum joint shear strength of 180 MPa is obtained for the joint brazed at 1193 K for 15 min under the present conditions. The intermetallic compound (Ti, Zr)<sub>2</sub>Cu distributed in the  $\alpha$ -Ti phase is harmful to the mechanical properties.

**Acknowledgements** This work was financially supported by the Key Project of Natural Science Foundation of Tianjin City (No. 14JCZDJC38600).

## References

- [1] Bao JW, Yang SY, Yang T. Microstructural evolution, tensile property and dynamic compressive property of FSWed Ti-6Al-4V alloy. *Rare Met.* 2020;39(2):169.
- [2] Wang QJ, Sun YL, Shuang YX, Wang W, Zhou HX. Aging-hardening behavior and phase transition kinetics of a novel beta-Ti Alloy. *Chin J Rare Met.* 2019;43(10):1103.
- [3] Ganjeh E, Sarkhosh H, Bajgholi ME, Khorsand H, Ghaffari M. Increasing Ti-6Al-4V brazed joint strength equal to the base metal by Ti and Zr amorphous filler alloys. *Mater Charact.* 2012; 71:31.
- [4] Pang SJ, Sun LL, Xiong HX, Chen C, Liu Y, Li H, Zhang T. A multicomponent TiZr-based amorphous brazing filler metal for high-strength joining of titanium alloy. *Scripta Mater.* 2016;117: 55.
- [5] Li L, Li XQ, Li ZF, Hu K, Qu SG, Yang C. Comparison of TiAl-based intermetallics joints brazed with amorphous and crystalline Ti-Zr-Cu-Ni-Co-Mo fillers. *Adv Eng Mater.* 2016; 18(2):341.



- [6] Hao YL, Li SJ, Yang R. Biomedical titanium alloys and their additive manufacturing. *Rare Met.* 2016;35(9):661.
- [7] Luo J, Wang LF, Li MQ, Ge CJ, Ma XX, Yang YT. Formation of adiabatic shear band and deformation mechanisms during warm compression of Ti-6Al-4V alloy. *Rare Met.* 2016;35(8):598.
- [8] Ganjeh E, Sarkhosh H. Microstructural, mechanical and fractographic study of titanium-CP and Ti-6Al-4V similar brazing with Ti-based filler. *Mater Sci Eng, A.* 2013;559:119.
- [9] Wang Y, Qiu QW, Yang ZW, Wang DP. Microstructure evolution and mechanical properties of Ti-43Al-9V-0.3Y alloy joints brazed with Ti-Zr-Ni-Cu + Mo composite filler. *Adv Eng Mater.* 2016;18(6):944.
- [10] Li L, Li XQ, Hu K, Qu SG, Yang C, Li ZF. Effects of brazing temperature and testing temperature on the microstructure and shear strength of  $\gamma$ -TiAl joints. *Mater Sci Eng, A.* 2015;634:91.
- [11] Chang CT, Shiue RK. Infrared brazing Ti-6Al-4V and Mo using the Ti-15Cu-15Ni braze alloy. *Int J Refract Met Hard Mater.* 2005;23(3):161.
- [12] Shiue RK, Wu SK, Chen YT, Shiue CY. Infrared brazing of Ti50Al50 and Ti-6Al-4V using two Ti-based filler metals. *Intermetallics.* 2008;16(9):1083.
- [13] Li XQ, Li L, Hu K, Qu SG. Vacuum brazing of TiAl-based intermetallics with Ti-Zr-Cu-Ni-Co amorphous alloy as filler metal. *Intermetallics.* 2015;57:7.
- [14] Liu YP, Wang G, Cao W, Xu HT, Huang ZJ, Zhu DD, Tan CW. Brazing ZrB<sub>2</sub>-SiC ceramics to Ti6Al4V alloy with TiCu-based amorphous filler. *J Manuf Process.* 2017;30:516.
- [15] Wang G, Huang YJ, Wang GC, Shen J, Chen ZH. Brazing of Ti<sub>2</sub>AlNb based alloy with amorphous Ti-Cu-Zr-Ni filler. *J Wuhan Univ Technol Mater Sci Ed.* 2015;30(3):61.
- [16] Chang CT, Du YC, Shiue RK, Chang CS. Infrared brazing of high-strength titanium alloys by Ti-15Cu-15Ni and Ti-15Cu-25Ni filler foils. *Mater Sci Eng, A.* 2006;420(1-2):155.
- [17] Szewieczek D, Tyrlik J. Designing the brazed joint properties with application of amorphous tape as a filler metal. *J Mater Process Technol.* 1995;53(1-2):405.
- [18] Liu YH, Hu JD, Zhang YP, Guo ZX, Yang Y. Joining of zirconia and Ti-6Al-4V using a Ti-based amorphous filler. *J Mater Sci Technol.* 2011;27(7):653.
- [19] Jing YJ, Yue XS, Gao XQ, Su DY, Hou JB. The influence of Zr content on the performance of TiZrCuNi brazing filler. *Mater Sci Eng, A.* 2016;678:190.
- [20] Li H, Zhao ZL, Guo HZ, Ning YQ, Yao ZK, Li K. Dependence of  $\alpha$ -phase size on flow stress during dynamic recrystallization steady state in Ti60 alloy. *Rare Met.* 2017;36(11):851.
- [21] Kang DH, Sun JH, Lee DM, Shin SY, Kim HS. Partially alloyed filler sheet for brazing of Ti and its alloys fabricated by spark plasma sintering method. *Mater Sci Eng, A.* 2009;527(1-2):239.
- [22] Elrefaey A, Tillmann W. Effect of brazing parameters on microstructure and mechanical properties of titanium joints. *J Mater Process Technol.* 2009;209(10):4842.
- [23] Chang CT, Wu ZY, Shiue RK, Chang CS. Infrared brazing Ti-6Al-4V and SP-700 alloys using the Ti-20Zr-20Cu-20Ni braze alloy. *Mater Lett.* 2007;61(3):842.
- [24] Yan HM, Liu Y, Pang SJ, Zhang T. Glass formation and properties of Ti-based bulk metallic glasses as potential biomaterials with Nb additions. *Rare Met.* 2018;37(10):831.
- [25] Frick WR. *Brazing handbook.* Florida: American Welding Society. Miami. 1991. 535.
- [26] Kattner UR, Massalski TB. *Binary alloy phase diagrams.* Materials Park: ASM International. 1990. 147.
- [27] Qiu QW, Wang Y, Yang ZW, Hu X, Wang DP. Microstructure and mechanical properties of TiAl alloy joints vacuum brazed with Ti-Zr-Ni-Cu brazing powder without and with Mo additive. *Mater Design.* 2016;90:650.
- [28] Lee MK, Kim KH, Lee JG, Rhee CK. Growth of isothermally-solidified titanium joints using a multi-component Zr-Ti-Cu-Ni-Be amorphous alloy as a brazing filler. *Mater Charact.* 2013;80:98.
- [29] Botstein O, Schwarzman A, Rabinkin A. Induction brazing of Ti-6Al-4V alloy with amorphous 25Ti-25Zr-50Cu brazing filler metal. *Mater Sci Eng, A.* 1996;206(1):14.